Development 139, 1023-1033 (2012) doi:10.1242/dev.071555

Initiation of synapse formation by Wnt-induced MuSK endocytosis

Laura R. Gordon, Katherine D. Gribble, Camille M. Syrett and Michael Granato*

SUMMARY

In zebrafish, the MuSK receptor initiates neuromuscular synapse formation by restricting presynaptic growth cones and postsynaptic acetylcholine receptors (AChRs) to the center of skeletal muscle cells. Increasing evidence suggests a role for Wnts in this process, yet how muscle cells respond to Wnt signals is unclear. Here, we show that in vivo, *wnt11r* and *wnt4a* initiate MuSK translocation from muscle membranes to recycling endosomes and that this transition is crucial for AChR accumulation at future synaptic sites. Moreover, we demonstrate that components of the planar cell polarity pathway colocalize to recycling endosomes and that this localization is MuSK dependent. Knockdown of several core components disrupts MuSK translocation to endosomes, AChR localization and axonal guidance. We propose that Wnt-induced trafficking of the MuSK receptor to endosomes initiates a signaling cascade to align pre- with postsynaptic elements. Collectively, these findings suggest a general mechanism by which Wnt signals shape synaptic connectivity through localized receptor endocytosis.

KEY WORDS: Zebrafish, Muscle specific kinase, MuSK, Unplugged, Wnt11, Dishevelled, Rab11, Recycling endosome, Neuromuscular junction, Planar cell polarity, AChR pre-pattern, Motor axons

INTRODUCTION

Synapse formation requires the precise alignment of pre- and postsynaptic elements. In the case of neuromuscular synapses, this process involves proper navigation of motor axons from the spinal cord to their muscle targets as well as the spatial alignment of these motor axons with acetylcholine receptors (AChRs) on the muscle surface (reviewed in Wu et al., 2010). Neuromuscular synapse development can be subdivided into two functionally distinct phases: an early and a late phase (Flanagan-Steet et al., 2005; Panzer et al., 2006; Wu et al., 2010; Zhang et al., 2004). The late phase is characterized by the transformation of motor growth cones into presynaptic nerve terminals which release signals, including Agrin, that are essential for postsynaptic stabilization and maturation (Campanelli et al., 1991; Godfrey et al., 1984; Ruegg et al., 1992; Wu et al., 2010). By contrast, the early phase is independent of the nerve and nerve-derived factors (Lin et al., 2001; Yang et al., 2001; Yang et al., 2000). During the early phase, even before the arrival of motor axons, AChRs accumulate in the center of muscle cells, precisely where the first synapses will form in a process termed AChR pre-patterning (Lin et al., 2001; Yang et al., 2001). Importantly, 'blocking' AChR pre-patterning through temporal inactivation of the muscle-specific kinase (MuSK) does not eliminate the formation of functional, mature synapses (Jing et al., 2009). Instead of navigating the center of muscle cells, motor axons now invade lateral muscle cell territories where they form ectopic synapses, suggesting that events during the early phase of neuromuscular development determine where synapses will form (Jing et al., 2009).

Department of Cell and Developmental Biology, University of Pennsylvania. Philadelphia, PA, 19104-6058, USA.

*Author for correspondence (granatom@mail.med.upenn.edu)

Accepted 22 December 2011

The receptor tyrosine kinase MuSK is a key player in determining where along the muscle cell synapses will form (DeChiara et al., 1996; Glass et al., 1996). In both mice and zebrafish, MuSK is expressed in early postsynaptic muscle cells, and in embryos lacking MuSK, AChRs fail to cluster in the center of muscle cells, and motor axons invade lateral muscle territory they usually avoid (DeChiara et al., 1996; Lin et al., 2001; Yang et al., 2001; Zhang et al., 2004). Overexpression of MuSK is sufficient to establish muscle pre-patterning through ligand-independent autoactivation (Kim and Burden, 2008), and in zebrafish the secreted glycoprotein Wnt11r binds to the MuSK ectodomain, and functional knockdown of *wnt11r* leads to defects in AChR pre-patterning and motor axon guidance (Jing et al., 2009). Although these studies suggest that Wnt signals play a crucial role in vertebrate neuromuscular development, the functional requirement for Wnt has not been confirmed using genetic mutants, and the mechanism by which Wnt signals initiate synapse formation has not been established.

Here, we characterize null mutants for *wnt11r* and show that *wnt11r* and *wnt4a* are essential for triggering relocalization of the MuSK receptor from the cell membrane to recycling endosomes located in the center of early muscle cells beneath future synaptic sites. We provide compelling evidence that MuSK localization to recycling endosomes activates a signaling cascade best known for its role in mediating planar cell polarity (PCP). PCP components colocalize with the internalized MuSK receptor and inhibition of selective PCP components results in a reduction of AChR pre-patterning and axon guidance errors. We propose a model in which Rab11-mediated trafficking positions a signaling complex consisting of the MuSK receptor and PCP components to the center of muscle cells to initiate synapse formation.

MATERIALS AND METHODS

Ethics statement

All experiments were conducted according to an Animal Protocol fully approved by the University of Pennsylvania Institutional Animal Care and Use Committee (IACUC) on 2 February, 2011; protocol number 803446. Veterinary care is under the supervision of the University Laboratory Animal Resources (ULAR) of the University of Pennsylvania.

Fish strains and animal care

All embryos used in this study were raised at 28°C for the required amount of time. Wild-type fish used for experiments were TLF, and mutants used were *musk (unp)*^{tbr307}(Zhang and Granato, 2000; Zhang et al., 2004), *wnt11r*$^{fh224(G94*)}$(Banerjee et al., 2011) and Tg*(mnx1:GFP)ml2* (Flanagan-Steet et al., 2005). Transgenic fish were used alone, in combination with each other or in combination with various mutant backgrounds.

Whole-mount immunocytochemistry and microscopy

Embryos were fixed and stained as described previously (Zeller et al., 2002) and labeling of AChRs was achieved via the method described by Jing et al. (Jing et al., 2009). The following antibodies and dilutions were used: znp-1 [1:200, Developmental Studies Hybridoma Bank (DSHB)], myc (9E10, 1:1000, Covance), F59 (1:20, DSHB). Embryos were imaged with LCS (Leica) and IX81 (Olympus) confocal microscopes.

Quantification of puncta, AChR clusters and RNA-injection membrane intensity

For puncta and AChR counts, confocal images were projected into a single plane and converted to a 16-bit image using Metamorph (Molecular Devices). Puncta were counted using the 'count nuclei' function, with the following parameters for each condition: AChRs imaged at 20× magnification, AChRs imaged at 60× magnification and endocytosed puncta imaged at 60× magnification with minimum/maximum lengths of 5/30, 5/100 and 1/10, respectively, and minimum average intensities of 30, 50 and 100, respectively. The results were imported to Microsoft Excel and Graphpad Prism for statistical analysis and plotting. Single confocal slices of images of RNA-injected embryos were converted to 16-bit images using Metamorph, and the maximum pixel intensity at three membranes per image was recorded manually for both color channels.

Whole-mount in situ hybridization

Colorimetric in situ hybridization was performed as described by Schneider and Granato (Schneider and Granato, 2006) with the previously published *wnt4a* in situ probe 'eu648' (Thisse and Thisse, 2005) and the previously published full-length *wnt11r* probe (Jing et al., 2009).

DNA, RNA and morpholino injections

Destination vectors containing either *GFP*- or *myc*-tagged constructs were microinjected into one-cell-stage embryos as previously described (Thermes et al., 2002). *wnt11r*, *unplugged-GFP* and *unpluggedΔCRD-GFP* mRNA were in vitro transcribed from *Not*I-linearized PCS2+ expression vectors using SP6 mMessage mMachine Kit (Ambion), diluted in 0.1 M KCl and microinjected into embryos at the one-cell stage. A previously published *wnt4a* translation-blocking morpholino (Matsui et al., 2005) targeting the following sequence was injected (7.2 ng) at the one-cell stage: CTCCGATGACATCTTTAGTGGAATC.

Plasmid construction

Rab11a-GFP and *rab11*(S25N) in PCS2+ (Clarke et al., 2006) were gifts from Clare Buckley (Kings College London, London, UK) and Gwyn Gould (University of Glasgow, Glasgow, UK). *mDiversin* in eYFP C1 was a gift from Tobias Schäfer (University Hospital Freiburg, Freiburg, Germany) (Haribaskar et al., 2009). *Daam1*-GFP in PCS2+ was a gift from Raymond Habas (Temple University, Philadelphia, PA, USA) (Liu et al., 2008). *XDishevelled*-GFP in PCS2+ was a gift from Peter Klein (University of Pennsylvania, PA, USA), *dishevelled*(DEP+) was cloned as previously described (Jing et al., 2009) and *dishevelled*(DIX) was subcloned from the full length construct using the following primers: AAAAGAATTCGCCACCATGGCGGAGACTAAAGTGATTTAC (forward) and AAAAAGAATTCTTAGAGCTCTCTGACCTCTGTAGCAGF (reverse). *NDaam1*-HA in pcDNA3 was a gift from Yasuyuki Kida (Tohoku University, Japan) (Kida et al., 2007). *CamKII*(K42M) and *rhoA*(N19) in pCS2+ were gifts from Juan Carlos Izpisua Belmonte (Salk Institute, CA, USA) (Matsui et al., 2005). *Unplugged*, *unpluggedΔ*CRD (Jing et al., 2009) and *wnt11r* were amplified from genomic DNA and cloned into the PCS2+ vector. Once cloned into PCS2+ (or in the case of *diversin-YFP* and *daam1b* in eYFP C1 and pcDNA3 vectors, respectively), the constructs were tagged with either GFP or 5×Myc using standard cloning procedures. Fusion constructs were PCR amplified from PCS2+ and cloned into pENTR/D-TOPO (Invitrogen, USA) using the following primers: 5′-CACCCAAGCTACTTGTTCTTTTTGC-3′ (forward) and 5′-GGTACCGGGCCCCAATGCATT-3′ (reverse). Constructs were then transferred to a homemade Gateway destination vector containing either the *3.8unp* promoter (below) or the *smyhc1* promoter using the Gateway LR Clonase II enzyme mix (Invitrogen, USA). The *3.8unp* promoter, which includes the 5′UTR and first intron of *musk*, was amplified from Fosmid CH1073-179D18 (BACPAC Resources, Oakland, CA, USA) using primers 5′-TGGTCTTTCGTGGAGTTC-3′(forward) and 5′-TGGTTGTGAGAAGTAAAGATCTG-3′ (reverse).

Chimeric embryos

Cell transplants were performed as described previously (Zeller and Granato, 1999) with the modification that embryos were fixed at 20 somites, permeabilized for 5 minutes with 0.1% collagenase, stained for 1 hour with fluorescently conjugated bungarotoxin and mounted in Vectashield for confocal imaging.

RESULTS

wnt11r and *wnt4a* are required for synaptic development

We reported previously that Wnt11r binds the MuSK receptor and that morpholino-mediated knockdown of *wnt11r* recapitulates the pre- and postsynaptic defects observed in *musk (unp)*-null mutants (Jing et al., 2009). These results suggest that Wnt11r is a ligand for MuSK, yet the incomplete phenotypic penetrance observed in *wnt11r* morphants left open the possibility of a partial morpholino knockdown, maternal contribution and/or additional ligands. To distinguish between these possibilities, we characterized AChR pre-patterning and axon guidance in embryos carrying an early stop codon in *wnt11r*, likely to represent a *wnt11r*-null allele (G94*) (Banerjee et al., 2011). Prior to the arrival of motor axons (20-somite stage), AChR clusters accumulate in a very narrow area in the center of individual muscle fibers (Fig. 1A). By contrast, in *wnt11r* mutants AChR clusters occupied a much broader area (~61% of hemisegments; Fig. 1E, quantified in 1L) or completely failed to accumulate AChRs to the muscle center (~39% of hemisegments; Fig. 1F). This failure to accumulate AChR clusters was observed in 100% of *musk (unp)* mutant hemisegments (Fig. 1C). Importantly, overall muscle morphology in *wnt11r*-null mutants was indistinguishable from wild-type siblings (supplementary material Fig. S1A,B).

Analysis of motor axons at 26 hours post fertilization (hpf) revealed that in *wnt11r* mutants, motor axons branched and invaded the lateral muscle territories from which they are excluded in wild-type embryos (Fig. 1G; *n*=338, ~26% of hemisegments), identical to the phenotype observed in *musk (unp)* mutants (Fig. 1D; *n*=148, ~85% of hemisegments). To test whether maternally provided *wnt11r* function might account for the quantitatively weaker pre- and postsynaptic phenotypes [compared with *musk (unp)* mutants], we examined mutant embryos derived from homozygous mutant *wnt11r* parents. These embryos displayed AChR and axonal phenotypes at frequencies very similar to those derived from *wnt11r* heterozygote parents (23% guidance defects in mutants derived from a heterozygote cross compared with 26% in mutants from a homozygote mutant cross; *n*=100 and *n*=338, respectively), suggesting that maternal *wnt11r* contributions are dispensable for synapse initiation. Thus, *wnt11r*-null mutants recapitulate the pre- and postsynaptic defects observed in *musk (unp)* null mutants (Fig. 1C,D), albeit with lower penetrance, suggesting the existence of additional MuSK ligands.

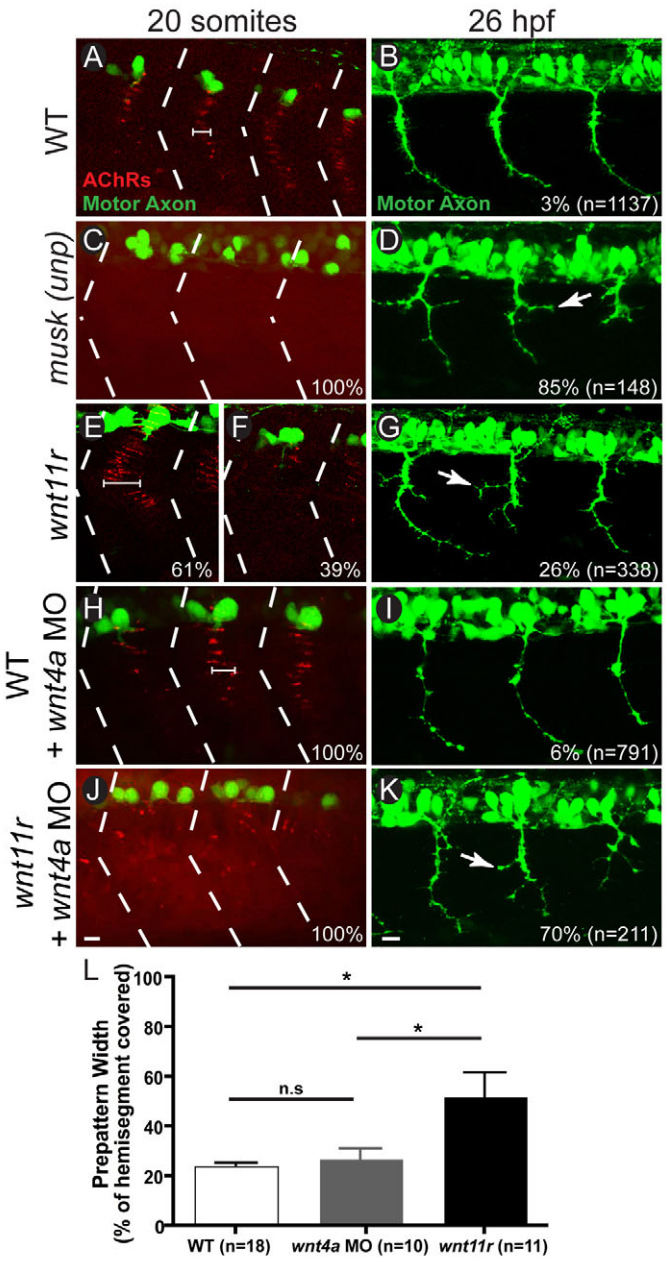

Fig. 1. Loss of *wnt11r* and *wnt4a* phenocopies *musk (unp)* mutant. (A-K) Lateral view of trunk (top, dorsal; left, anterior) stained for AChR clusters (bungarotoxin, red) and motor axons (znp-1, green) in 20-somite and 26 hpf zebrafish embryos. (**A**,**B**) Three hemisegments in a wild-type embryo (hemisegment boundaries marked with dashed lines) with pre-patterned AChR clusters along the center of each hemisegment (cluster width marked by bracket; A) and three wild-type hemisegments in which motor axons have made synaptic contacts along the length of the trunk (B). (**C**,**D**) Three hemisegments in a *musk (unp)* mutant showing the absence of clustered AChRs, resulting in a complete dispersion of AChRs (C) and axon guidance errors in 26 hpf *musk (unp)* mutants (arrow points to axon branch) which occur in 85% of axons (D). (**E-G**) A single hemisegment from a *wnt11r* embryo showing an expanded AChR pre-pattern (width bracketed, 61% occurrence; E), and a single hemisegment showing a complete loss of AChR pre-pattern (39% of occurrence; F). Three hemisegments in a 26 hpf *wnt11r* mutant showing *musk (unp)*-like axon branching (arrow) in 26% of axons (G). (**H**,**I**) Three hemisegments in a wild-type embryo injected with 10 ng of *wnt4a* morpholino showing wild-type-like pre-patterning (H) and wild-type-like axons with only 6% guidance errors (I). (**J**,**K**) Three hemisegments from a *wnt11r* mutant injected with 10 ng of *wnt4a* morpholino showing *musk (unp)*-like AChR dispersal in all hemisegments (J) and guidance errors in 70% of axons (K). (**L**) Quantification of increase in AChR pre-pattern width in *wnt11r* mutants compared with wild type or *wnt4a* morpholino injected (P=0.01 for wild type vs *wnt11r* mutant, P=0.02 for *wnt11r* mutant vs *wnt4a* morpholino injected and P=0.38 for wild type vs *wnt4a* morpholino injected; Student's two-tailed t-test, unequal variance; error bars indicate s.e.m.). Scale bars: 10 μm.

Given the great extent of redundancy among vertebrate Wnts, we hypothesized that other Wnts might be compensating in the absence of *wnt11r*. Based on its mRNA expression pattern in the vicinity of muscle cells that first form the AChR pre-pattern, we focused on *wnt4a* (supplementary material Fig. S1E,F). Using a previously characterized translation-blocking morpholino (Matsui et al., 2005), we found that knockdown of *wnt4a* by itself did not produce detectable perturbations of AChR pre-patterning or axon guidance (Fig. 1H,I). By contrast, injection of the same dose of *wnt4a* morpholino into *wnt11r* mutants exacerbated the partial *wnt11r*-null phenotype. In all *wnt11r*/*wnt4a*-deficient somitic segments, AChR receptors failed to accumulate in the center and instead formed small aggregates randomly along muscle fibers (Fig. 1J). These aggregates resemble AChR 'hot spots' known to form spontaneously along aneural muscle cells (Fischbach and Cohen, 1973; Sytkowski et al., 1973). Concomitantly, in 70% of *wnt11r*/*wnt4a*-deficient somitic segments, motor axons displayed *musk (unp)*-like branching defects (Fig. 1K), again without affecting overall muscle cell morphology (supplementary material Fig. S1C,D). Thus, loss of *wnt11r* and *wnt4a* mimics the AChR pre-pattern and axonal defects observed in *musk (unp)*-null mutants (Zhang and Granato, 2000), consistent with the idea that, in vivo, AChR pre-pattern requires the MuSK receptor and multiple Wnt ligands.

wnt11r regulates the level of membrane-bound MuSK

We next investigated how *wnt11r* and *wnt4a* initiate synapse formation. We had shown previously that ubiquitous expression of MuSK-Myc along the entire length of muscle cells did not alter the centrally localized AChR pre-pattern (Jing et al., 2010), suggesting that additional factors or processes might determine where along the muscle cell MuSK signals. In the early zebrafish embryo, Wnts recruit the Frizzled receptor and the obligate intracellular signaling component Dishevelled to the plasma membrane, thereby generating local cell contacts important for gastrulation movements (Witzel et al., 2006). To test whether Wnts might alter the cellular distribution of MuSK, one-cell-stage embryos were injected with mRNAs encoding GFP-tagged MuSK and the membrane marker mCherry-CAAX, in the absence or presence of *wnt11r* mRNA. Four and a half hours later, at dome stage, injected embryos were analyzed for the cellular localization of MuSK-GFP protein (Fig. 2). Importantly, these early embryos do not express *wnt11r* endogenously, providing a 'Wnt-naive' environment (Nojima et al., 2010).

In the absence of *wnt11r* mRNA, MuSK-GFP is highly enriched at the cell membrane, as expected for a receptor tyrosine kinase (Fig. 2A-A″). By contrast, in the presence of

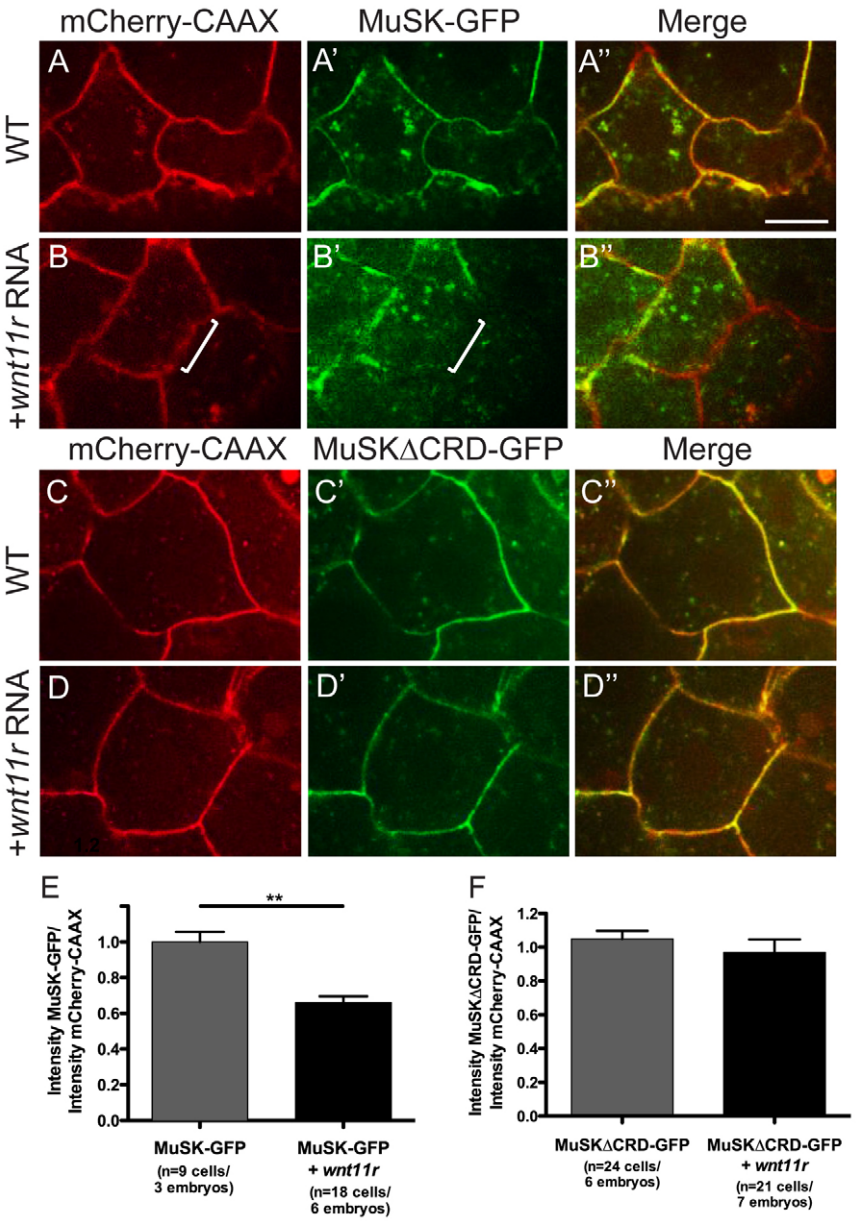

Fig. 2. Addition of *wnt11r* triggers a loss of MuSK-GFP at the membrane in a CRD-dependent manner. (**A-D″**) Dome-stage zebrafish embryos at 4.5 hpf expressing mCherry-CAAX membrane marker (red) and either MuSK-GFP or MuSKΔCRD-GFP (green) in separate and merged channel views. (A-A″) Wild-type embryos showing MuSK-GFP membrane localization. (B-B″) Wild-type embryos injected with *wnt11r* mRNA showing reduced MuSK-GFP at the membrane (white bracket highlights one area of reduced GFP signal). (C-C″) Wild-type embryos showing MuSKΔCRD-GFP expression at the membrane, which is not reduced in the presence of *wnt11r* mRNA (D-D″). (**E**) Quantification of effect of *wnt11r* on MuSK-GFP membrane localization (**P=4.6×10^{-5}; Student's two-tailed *t*-test, unequal variance). (**F**) Quantification of effect of *wnt11r* on MuSKΔCRD-GFP membrane localization (P=0.39; Student's two-tailed *t*-test, unequal variance). Error bars represent s.e.m. Scale bar: 10 μm.

wnt11r mRNA, levels of MuSK-GFP at the cell membrane were dramatically reduced (Fig. 2B-B″, quantified in 2E). Moreover, deletion of the cysteine-rich domain (CRD), which is essential for Wnt11r binding to the MuSK-GFP ectodomain (Jing et al., 2010), did not affect steady-state membrane levels of MuSK-GFP in the absence of *wnt11r* (Fig. 1C-C″), but reduced *wnt11r* responsiveness (Fig. 1D-D″, quantified in 1F). These data demonstrate that exposure to *wnt11r* alters membrane localization of MuSK, suggesting that Wnt11r affects MuSK protein stability or dynamics, possibly by modulating localization at the plasma membrane.

MuSK-GFP localization to recycling endosomes 'marks' the site of future synapses

To explore the relationship between Wnt exposure and MuSK localization in the relevant cellular context, we examined MuSK localization in early muscle cells, the adaxial muscle cells, which, in the zebrafish embryo, form the first AChR pre-pattern. *musk* mRNA is detectable prior to and during the time period of AChR pre-patterning in adaxial muscle cells and becomes undetectable soon afterwards (Zhang et al., 2004). To express *musk* in adaxial muscle cells, we cloned 3.8 kb of genomic DNA directly upstream of the *musk* translational start site (*3.8unp*) and used this to drive the expression of *GFP* or *musk-GFP*.

Injection of *smyhc1:GFP*, a bona fide promoter for adaxial muscle (Elworthy et al., 2008), or the *3.8musk* promoter driving *GFP*, resulted in GFP expression throughout the cytoplasm of stochastically labeled wild-type adaxial muscle cells (Fig. 3A,B). Stochastic labeling results in individual cells that retain and express the injected DNA construct, surrounded by cells which do not retain the DNA and hence do not express the construct (Downes et al., 2002). Injection of *3.8musk* driving *musk-GFP* (*3.8musk*:MuSK-GFP) into *musk (unp)*-null mutant embryos restored AChR pre-patterning, demonstrating that this construct is functional (supplementary material Fig. S2B,B′). Injection of *3.8musk*:MuSK-GFP into wild-type embryos resulted in stochastic

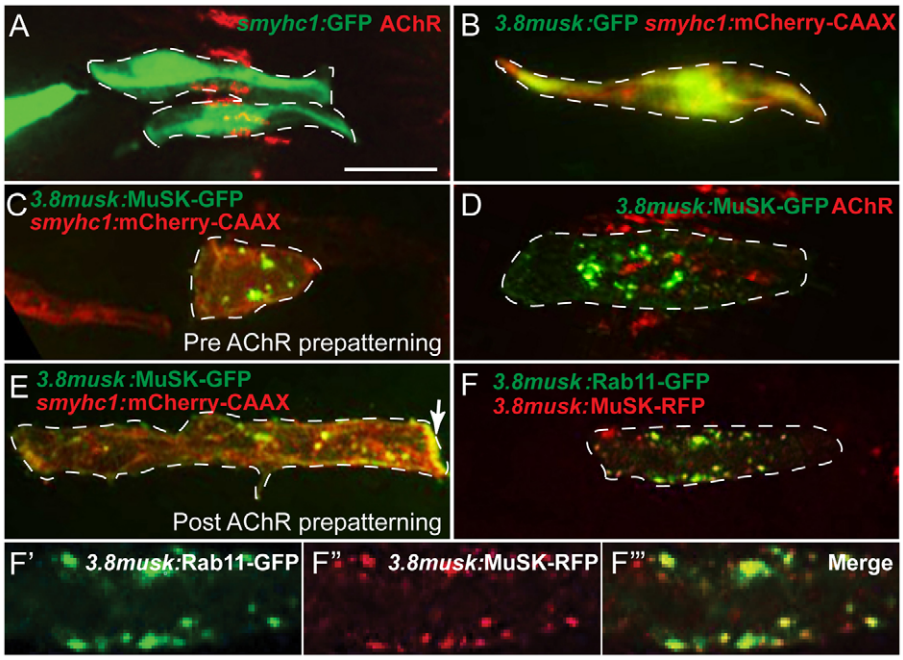

Fig. 3. MuSK-GFP localizes to Rab11-positive endosomes in the center of presynaptic muscle cells. (**A**) Expression of GFP driven by the *smyhc1* promoter in two wild-type adaxial muscle cells (green) with pre-patterned AChR clusters (bungarotoxin, red) along the center of adaxial muscle cells. (**B**) Expression of *3.8musk*:GFP (green) and membrane marker *smyhc1:mCherry-CAAX* (red) in an individual adaxial muscle cells. (**C**) *3.8musk*:MuSK-GFP (green) and *smyhc1:mCherry-CAAX* (red) in a 'young' adaxial muscle cell that does not yet have pre-patterned AChR clusters. (**D**) *3.8musk*:MuSK-GFP in an adaxial muscle cell (green) with AChRs (bungarotoxin, red) showing that MuSK-GFP puncta aggregate in close proximity to pre-patterned AChR clusters. (**E**) *3.8musk*:MuSK-GFP (green) and *smyhc1:mCherry-CAAX* (red) in an 'older' adaxial muscle cell that no longer has pre-patterned AChRs, showing a reduction in central MuSK-GFP puncta (accumulation of protein at the myoseptal boundary is marked with an arrow). (**F-F‴**) A single confocal slice showing colocalization of MuSK-RFP (red) and early/recycling endosome marker Rab11-GFP (green) expressed under the *3.8musk* promoter in a normal view (F) and magnified views (F-F″). Dashed lines encircle a single muscle cell. Scale bar: 10 μm.

expression of the fusion protein in adaxial muscle cells, but unlike expression of only GFP under the same promoter, MuSK-GFP localized to puncta in the center of adaxial muscle cells before and during the time period of AChR pre-patterning, but not post-AChR pre-patterning, when these cells undergo a medial-to-lateral migration (Flanagan-Steet et al., 2005) (Fig. 3C-E). Live imaging revealed that these MuSK-GFP-positive puncta were highly dynamic and that they appeared to be actively maintained in the muscle center, as puncta that strayed from the center rapidly moved back to the central position (supplementary material Movie 1).

To determine whether these puncta consist of cytoplasmic protein aggregates or whether they represent a regulated pool of endocytosed protein, we co-injected into wild-type embryos *3.8musk*:MuSK-RFP with *rab7-GFP*, a late endosome marker, and *rab11-GFP*, a marker for exocytic/recycling endosomes (reviewed by Hutagalung and Novick, 2011). Rab7-positive endosomes were present throughout the entire length of individual adaxial muscle cells, and only a very small fraction of Rab7-positive endosomes colocalized with MuSK (supplementary material Fig. S2D-D″). Conversely, Rab11-positive vesicles were restricted to the central portion along the anterior-posterior axis of both wild-type and *musk (unp)* mutant muscle cells, and the majority colocalized with MuSK (Fig. 3F-F‴, quantified in supplementary material Fig. S2G). Thus, MuSK expressed under its endogenous promoter localizes just before and during the time of AChR pre-patterning to Rab11-positive vesicles at the center of adaxial muscle, precisely where AChRs accumulate.

MuSK-GFP accumulation in endosomes depends on *wnt11r* and *wnt4a*

Rab11 is a member of the large family of small GTPases, and regulates both the exocytic biosynthetic and the recycling pathway (Chen et al., 1998; Ren et al., 1998; Satoh et al., 2005; Sonnichsen et al., 2000; Ullrich et al., 1996). To determine whether MuSK localization to exocytic/endocytic vesicles depends on *rab11* function, we expressed a dominant-negative, GDP-restricted *rab11*, *rab11*(S25N) (Ren et al., 1998), stochastically in adaxial muscle cells. To ensure high levels of expression that are essential for maximal efficacy of dominant-negative proteins, we used the 'stronger' *smyhc1* adaxial promoter rather than the weak *3.8unp* promoter. As shown in Fig. 4, disruption of *rab11* function resulted in uniform MuSK-RFP distribution along the entire length of adaxial muscle cells, suggesting that MuSK protein localization depends on *rab11*-mediated trafficking (Fig. 4A,A′, quantified in 4E). Importantly, Rab11 localization is unaffected in *musk (unp)* mutant adaxial cells (supplementary material Fig. S2G). Similarly, 'global' overexpression of wild-type *rab11*-GFP via mRNA injection or high level expression of wild-type *rab11*-GFP in individual muscle cells via the *smyhc1* promoter did not perturb AChR pre-patterning or *musk-mKate* localization (supplementary material Fig. S2E-F′; data not shown).

If the localization of MuSK to Rab11-positive vesicles is functionally important for *wnt11r*- and *wnt4a*-induced synapse initiation, then several predictions can be made. First, the disruption of *rab11*-mediated processes in adaxial muscle cells should affect AChR pre-patterning and motor axon guidance. Indeed, when we expressed *rab11*(S25N)-*myc* in individual adaxial muscle cells, we

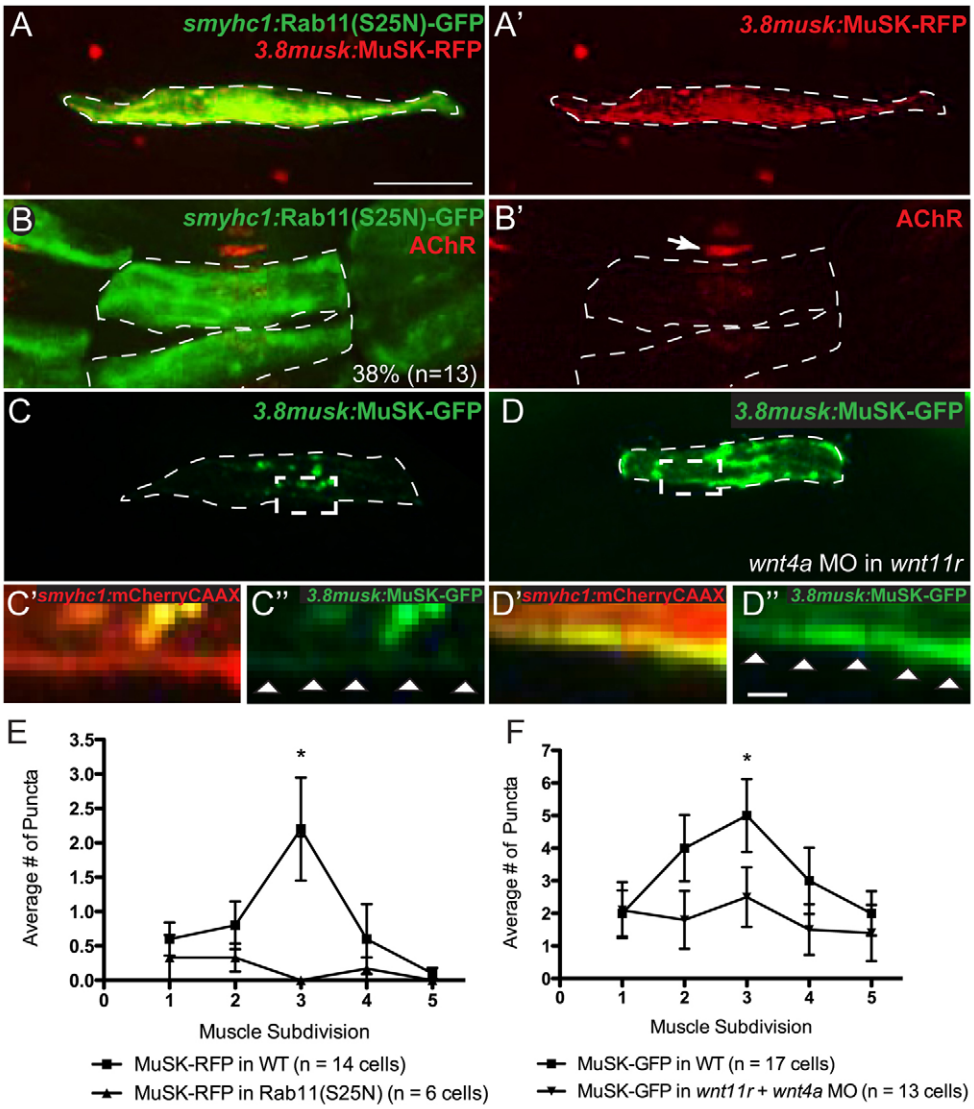

Fig. 4. MuSK trafficking is disrupted in the absence of *rab11* and *wnt11r/4a*. (**A**,**A′**) Co-expression of *smyhc1:rab11*(S25N)-*GFP* (green) and *3.8musk*:MuSK-RFP (red; alone in A′), demonstrating disruption of MuSK-RFP center muscle localization. Instead, MuSK-RFP appears dispersed throughout the cell. (**B**,**B′**) *smyhc1:rab11*(S25N)-*GFP* (green) expressed in two adjacent muscle cells showing disruption of AChR clusters (bungarotoxin, red) at the interface of the two mosaic fibers but not in an adjacent wild-type cell (arrow). Observed in 38% of cell interfaces, *n*=13. (**C-C″**) *3.8musk*:MuSK-GFP (green) in a wild-type embryo with normal protein distribution (C) and a magnified view of dashed box showing very little protein at the membrane as visualized with *smyhc:mCherryCAAX* (C′,C″). (**D-D″**) *3.8musk*:MuSK-GFP (green) in a *wnt11r* mutant/*wnt4a* morphant embryo (D), and magnified view of dashed box showing accumulation of protein at the membrane as visualized with *smyhc:mCherryCAAX* (D′,D″). (**E**,**F**) Quantification of central enrichment of MuSK-RFP puncta when co-expressed with Rab11(S25N)-GFP (E) (*P* values for muscle subdivisions 1-5: 0.6, 0.27, 0.01, 0.38, 0.34, respectively), or when expressed in a *wnt11r* mutant/*wnt4a* morphant background (F; *P* values for muscle subdivisions 1-5: 0.87, 0.12, 0.04, 0.36, 0.97, respectively). **P*<0.05. Error bars represent s.e.m. Dashed lines encircle a single muscle cell. Arrowheads (C″,D″) indicate cell membrane. Scale bars: 10 μm in A-D; 1 μm in C′-D″.

observed a decrease in AChR clustering in these cells but not in the surrounding wild-type cells (38%, *n*=13 cells in five embryos; Fig. 4B,B′). Similarly, expression of *rab11*(S25N)-myc in individual muscle cells resulted in *musk (unp)*-like axonal defects in 32% of hemisegments (*n*=50).

A second prediction is that in the absence of Wnt signals, the subcellular localization of MuSK to recycling endosomes would be affected. Consistent with our findings that AChR pre-patterning requires both *wnt11r* and *wnt4a* function (Fig. 1), analysis of *wnt11r* mutant/*wnt4a* morphant embryos revealed a nearly complete shift in the subcellular localization of MuSK-GFP from Rab11-positive vesicles to the cell membrane (Fig. 4C-C″,D-D″, quantified in 4F). These results demonstrate that Wnt signaling is required to traffic MuSK-GFP from the cell membrane into Rab11-positive vesicles. Moreover, the accumulation of MuSK-GFP at the cell membrane of *wnt11r* mutant/*wnt4a* morphant embryos strongly argues that MuSK-GFP and Rab11 double-positive vesicles are not exocytic vesicles, but do indeed represent recycling endosomes. Combined, our data show that *wnt11r*- and *wnt4a*-dependent trafficking of MuSK from the cell membrane to Rab11-positive endosomes is essential for AChR pre-patterning.

Functional interdependence of PCP core proteins with MuSK-GFP

Given the striking subcellular localization of MuSK-GFP in response to Wnt signals, we examined the localization of several components of the noncanonical Wnt signaling pathway. We previously used a dominant-negative version of *dishevelled*, *dishevelled*(DEP+), that specifically blocks noncanonical Wnt signaling (Axelrod et al., 1998; Heisenberg et al., 2000; Jing et al., 2009; Wallingford et al., 2000), to demonstrate that *dishevelled*-dependent noncanonical signaling in adaxial muscle is crucial for restricting AChR clusters and motor axons to the central portion of adaxial muscle cells. Although it is known that Dishevelled can bind the juxtamembrane/kinase domain of the MuSK receptor (Luo et al., 2002), the subcellular localization of Dishevelled and other PCP core components during vertebrate neuromuscular synapse formation has not been established. To examine the subcellular localization of PCP core components, we expressed Daam1-GFP, Ankrd6-YFP and Dishevelled-GFP in individual adaxial muscle cells and examined their localization just prior to and during the period of AChR pre-patterning. To avoid nonspecific protein aggregates, we used the *3.8musk* promoter, which drives protein

expression at much lower levels than the 'stronger' *smyhc1* promoter. Indeed, expression of most PCP core proteins under the control of the *smyhc1* promoter resulted in nonspecific protein aggregates (data not shown).

Confocal analysis revealed that Daam1-GFP, Ankrd6-YFP and Dishevelled-GFP localize to vesicle-like puncta that are strongly enriched in the central region of adaxial muscle cells, identical to the localization of MuSK-GFP (Fig. 5A-C, quantified in supplementary material Fig. S3A). Moreover, stochastic expression of a dominant-negative version of *daam1* (*NDaam1*) (Kida et al., 2007) and *rhoA* [*rhoA*(N19)] (Matsui et al., 2005) in adaxial muscle cells reduced AChR pre-patterning and caused *musk (unp)*-like axonal guidance defects, confirming that PCP pathway components play a crucial role in this process (supplementary material Fig. S3E,F,I-J′). Importantly, blocking the canonical Wnt pathway or the Wnt/Ca^{2+} pathway did not affect AChR clustering or axon guidance (supplementary material Fig. S3C,D,G-H′). Finally, co-expression of *dishevelled-GFP* and *musk-mKate* revealed a high degree of colocalization between both proteins, strongly suggesting that in adaxial muscle cells, PCP core components such as Dishevelled associate with recycling endosomes (Fig. 5E-E″).

In *Drosophila*, PCP core components are dependent on one another for their correct subcellular localization. For example, loss of one PCP core component, such as the *frizzled* receptor, disrupts localization of other core proteins (reviewed in Wu and Mlodzik, 2009). The analogous prediction for this system would be that blocking the MuSK receptor should interfere with Dishevelled-GFP localization, and vice versa. Remarkably, the subcellular localization of Dishevelled-GFP to the center of adaxial muscle cells is completely abolished in *musk (unp)* mutants, and instead Dishevelled-GFP is diffusely distributed throughout the cytoplasm (Fig. 5C,D, quantified in 5H). Conversely, blocking *dishevelled*-dependent noncanonical signaling in adaxial muscle cells leads to a significant redistribution of MuSK-GFP from the endosomal compartment in the muscle center to the cell membrane (Fig. 5F-G″), identical to what we observed when blocking *wnt11r* and *wnt4a* function (Fig. 4D-D″). Importantly, localization of Rab11-GFP is independent of *dishevelled* function, suggesting that *rab11* probably functions 'upstream' of *dishevelled*, and that the dependence of MuSK localization on *dishevelled* is highly specific (supplementary material Fig. S2G). Thus, several core PCP proteins colocalize with MuSK to presumptive endosomal organelles in the center of adaxial muscle cells, precisely where the AChR pre-pattern forms.

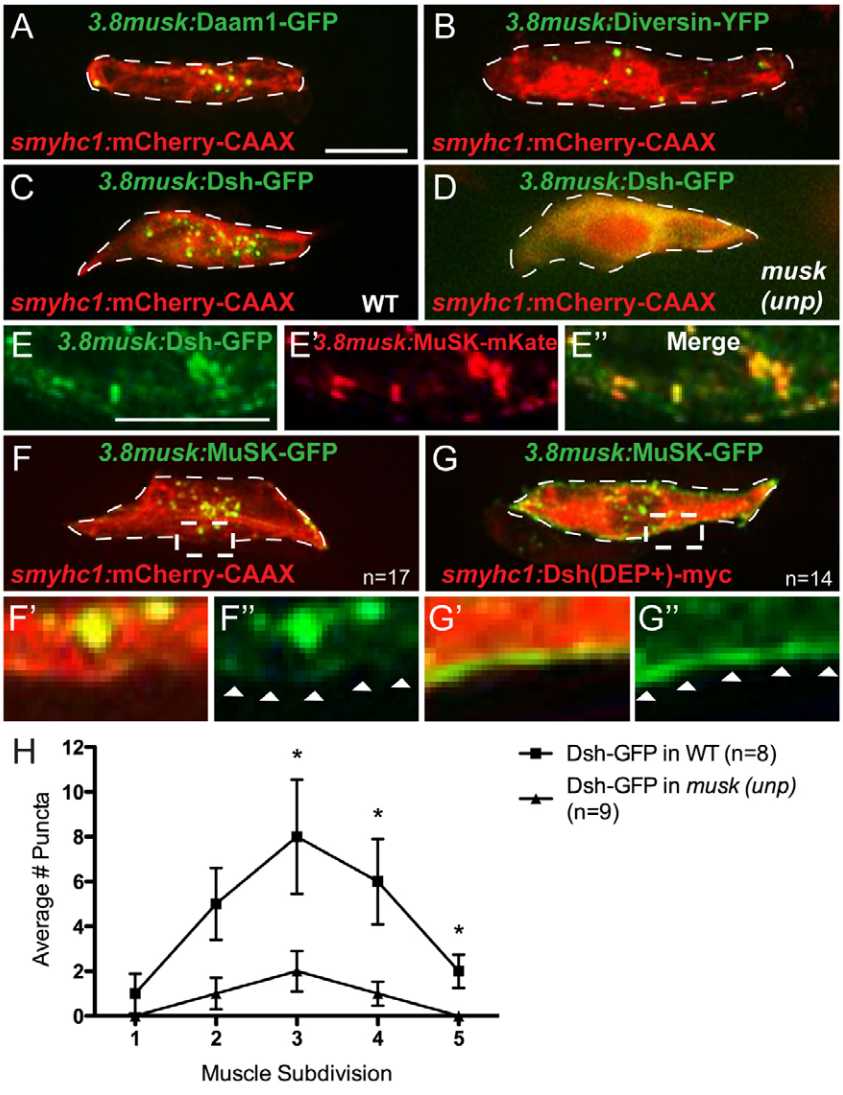

Fig. 5. Localization of noncanonical PCP proteins to the center of muscle cells requires MuSK, and vice versa. (**A**,**B**) Daam1-GFP (green) (A) and Diversin-YFP (green) (B) under the *3.8musk* promoter localize to centrally enriched puncta in muscle cells co-expressing mCherry-CAAX under the *smyhc1* promoter (red). (**C**) Dsh-GFP under the *3.8musk* promoter (green) localizes to centrally enriched puncta in fibers co-expressing mCherry-CAAX (red). (**D**) The punctate localization of Dsh-GFP (green) is lost in *musk (unp)* mutant muscle cells (mCherry-CAAX in red). (**E-E″**) Magnified view of center of muscle cell showing colocalization of Dsh-GFP (green) and MuSK-mKate (red), both driven by the *3.8musk* promoter. (**F-F″**) MuSK-GFP under the *3.8musk* promoter (green) localizes to centrally enriched puncta in muscle cells co-expressing mCherry-CAAX (red). F′ and F″ show magnified views of the region marked with dashed box in F. (**G-G″**) MuSK-GFP localizes to the membrane of muscle cells co-expressing Dsh(DEP+)-Myc. G′ and G″ show magnified views of the region marked with dashed box in G. (**H**) Quantification of reduction in centrally localized Dsh-GFP puncta in *musk (unp)* mutants (*P* values for muscle subdivisions 1-5: 0.49, 0.09, 0.05, 0.04, 0.02, respectively). **P*<0.05. Error bars represent s.e.m. Dashed lines encircle a single muscle cell. Arrowheads in F″ and G″ indicate cell membrane. Scale bars: 10 μm.

Moreover, MuSK and Dishevelled are dependent on one another for proper localization, consistent with the idea that both participate in a PCP-like signaling cascade to initiate synapse development.

DISCUSSION

Initiation of neuromuscular synapses depends on multiple Wnt signals

Genetic mutants and knockouts have demonstrated that Wnts play a crucial role in the assembly and plasticity of central synapses (Budnik and Salinas, 2011; Ciani and Salinas, 2005; Hall et al., 2000; Lucas and Salinas, 1997; Wu et al., 2010; Yang et al., 2010). Wnts are also involved at the invertebrate neuromuscular synapse (reviewed by Davis and Ghosh, 2007; Klassen and Shen, 2007). However, the situation at the vertebrate neuromuscular junction (NMJ) is less well defined. Mice mutant for the *frizzled* co-receptor *lrp4* lack all AChR pre-patterning and mature NMJ synapses (Kim, N. et al., 2008; Weatherbee et al., 2006; Zhang et al., 2008), and knockdown of zebrafish *wnt11r* significantly reduces AChR pre-patterning (Jing et al., 2009). Although these reports strongly suggest that Wnts are crucial for vertebrate neuromuscular synapse development, Wnt knockouts or genetic mutants with defects in neuromuscular synapse development have not yet been reported.

Here, we demonstrate that *wnt11r*-null mutants display profound pre- and postsynaptic defects during the early phase of synapse development, without obvious defects in muscle development. Interestingly, we find that only the combined inactivation of *wnt11r* and *wnt4a* results in a complete loss of AChR pre-patterning, almost identical to that observed in *musk (unp)* mutants (Fig. 1C,J). *Wnt11r* mRNA is expressed in the lateral mesoderm (Groves et al., 2005; Matsui et al., 2005) (supplementary material Fig. S1G,H), consistent with a paracrine mode of action, whereas *wnt4a* is expressed in adaxial muscle, suggesting an autocrine mode of operation (supplementary material Fig. S1E,F). At the *Drosophila* NMJ, Wg and Wnt5 function in a well-documented autocrine manner (Liebl et al., 2008; Packard et al., 2002) and future experiments are required to determine whether, in zebrafish, muscle-derived *wnt4a* activates the muscle-expressed MuSK receptor directly. Combined, our results uncover the first genetic requirement for Wnts during vertebrate NMJ synapse development and demonstrate that multiple Wnt signals initiate synapse formation.

MuSK receptor localization to recycling endosomes is crucial for synapse development

Once thought to terminate transmembrane receptor signaling, the endocytic pathway is becoming increasingly appreciated for its ability to activate signaling of surface receptors such as the Notch, EGF and Eph receptors (reviewed by Gagliardi et al., 2008; Pitulescu and Adams, 2010), as well as chemokine receptors such as Cxcr2. For example, it has been shown that in response to ligand stimulation, the Cxcr2 receptor is internalized into Rab11-positive recycling endosomes, and that reducing Cxcr2 recycling diminishes Cxcr2-mediated chemotaxis (Fan et al., 2004). Similarly, Wnt-mediated activation of Frizzled3 on axonal growth cones triggers Frizzled3 endocytosis and thereby initiates PCP signaling within growth cones (Shafer et al., 2011). This and other experiments have contributed to the current view that upon ligand binding, receptor endocytosis can lead to degradation or to signaling, depending on the endocytic compartment to which the receptor is sorted (reviewed in Gagliardi et al., 2008). In the case of receptor tyrosine kinases, there is accumulating evidence that receptor endocytosis is required for signal transduction (Jing et al., 1992; Vieira et al., 1996; Yang et al., 2005).

Previous studies have shown that in response to ligand stimulation, MuSK undergoes rapid endocytosis in cultured myoblasts (Zhu et al., 2008). We find that in vivo and during the time of synapse initiation, MuSK is internalized from the cell membrane into Rab11-positive endosomes, and that this process is dependent on *wnt11r* and *wnt4a*. Moreover, *rab11* function is important for proper MuSK protein localization and AChR pre-patterning, demonstrating the importance of endosome recycling to initiate MuSK-dependent processes (Fig. 4). Although we cannot exclude the possibility that *rab11* exerts its function directly on AChR trafficking, recycling of AChR receptors has been observed only at mature NMJs and only in response to muscle stimulation (Bruneau and Akaaboune, 2006; Martinez-Pena y Valenzuela et al., 2010), whereas at the stage of AChR pre-patterning when we examined *rab11*-dependent trafficking, NMJs have not yet formed. Combined with the observations that MuSK is crucial for localization of Dishevelled to presumptive endosomes, and that Dishevelled function in muscle cells is crucial for AChR pre-patterning and axon guidance (see below) (Jing et al., 2009), we favor the idea that *rab11* regulates primarily MuSK localization and function.

Finally, we showed previously that forcing MuSK expression throughout the entire surface of muscle cells did not alter synapse initiation or position, suggesting the existence of additional regulators (Jing et al., 2009). Our finding that MuSK internalization to endosomes spatially restricts MuSK function and, hence, positions AChR clusters to the muscle center explains our previous results and strongly suggests that MuSK internalization to the spatially restricted Rab11-positive endosomal compartment determines where along the muscle cell future synapses will form.

Endocytosis, planar cell polarity and the initiation of neuromuscular synapses

The localization of MuSK to Rab11-positive endosomes and the requirement of *rab11*-mediated trafficking for AChR pre-pattern initiation suggests that the signaling proteins downstream of MuSK might localize to and be active at Rab11-positive endosomes. In fact, we find that several core components of the PCP pathway, including Dishevelled, localize to the center of muscle cells, precisely where AChR clusters accumulate, and we find that Dishevelled localization is MuSK-dependent (Fig. 5C,D). Conversely, blocking *dishevelled* function affects membrane-bound MuSK, preventing it from internalizing to the endosomal compartment, which ultimately results in defects in AChR pre-patterning and motor axon guidance (Fig. 5F-G″) (Jing et al., 2009). This reciprocal functional dependency is intriguingly reminiscent of how the PCP pathway patterns *Drosophila* wing disc cells, although the precise mechanism initiating PCP signaling there is still unresolved (reviewed by Strutt and Strutt, 2009). Consistent with our results that intracellular trafficking plays a vital role in establishing cellular polarity are recent reports on the role of sec24b, a component of the COPII complex that is essential for intracellular endoplasmic reticulum (ER)-to-Golgi protein transport (Sato and Nakano, 2007). Genetic and biochemical analyses show that during mouse embryogenesis, sec24b plays a crucial role in establishing planar cell polarity through selective trafficking of Vangl2 (Merte et al., 2010; Wansleeben et al., 2010). Our results provide compelling evidence for a model in which Wnt ligands initiate a MuSK-dependent signaling cascade in Rab11-positive recycling endosomes, where core PCP components modulate the cytoskeleton to determine the precise location of future synapses along the anterior-posterior axis of muscle cells (Fig. 6).

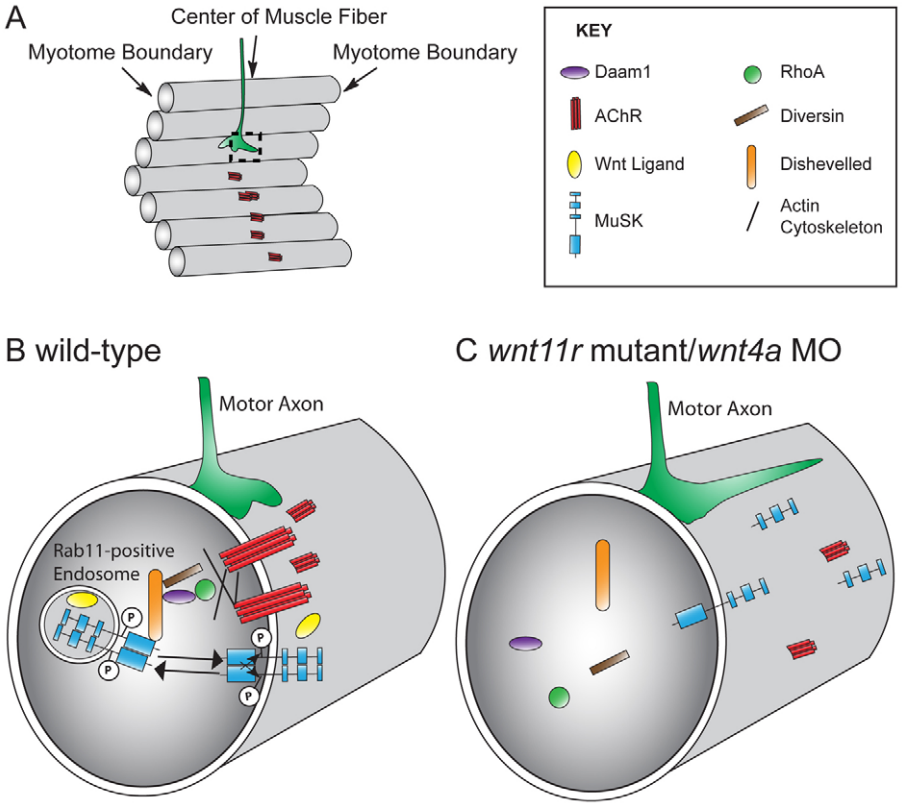

Fig. 6. Model for Wnt-dependent receptor endocytosis directing synapse position. (**A**) Schematic of a somitic hemisegment with parallel early muscle cells in gray. AChRs (red) are clustered in the center of the muscle fibers along the path where the motor axon (green) will extend. (**B**) Magnified view of dashed box in A showing a cross-section of a single wild-type muscle fiber. Motor axon growth cones (green) are navigating in the center of cells, precisely where AChRs (red) are clustered. In a Wnt ligand (yellow)-dependent manner, MuSK (blue) translocates from the membrane into Rab11-positive endosomes restricted to the center of muscle cells. It is unclear whether Wnt11r and Wnt4a directly activate the MuSK receptor in vivo or act indirectly on MuSK trafficking. Once internalized, the cytoplasmic domain of MuSK binds Dishevelled (orange) and nucleates accumulation of Diversin (Ankrd6; brown), Daam1 (purple) and RhoA (green) to modify the cytoskeleton, ultimately anchoring AChRs to the cell center. (**C**) Magnified view of showing a cross-section of a *wnt11r* mutant/*wnt4a* morphant muscle cell, in which MuSK, Dishevelled, Daam1, Diversin and RhoA are no longer localized in the center. Consequently, AChRs and growth cones (green) are no longer restricted to the muscle center.

Specifically, we propose a model (Fig. 6) in which secreted Wnt ligands, such as *wnt11r*, trigger translocation of the MuSK receptor from the cell surface into Rab11-positive recycling endosomes. Importantly, these endosomes are enriched and actively maintained in the center of the muscle fiber. Once endocytosed, MuSK associates with Dishevelled (Luo et al., 2002), which is known to stimulate signaling following Wnt-induced receptor endocytosis (Chen et al., 2003; Gao and Chen, 2009). For example, upon *wnt11*-mediated endocytosis of the Frizzled receptor, Dishevelled triggers noncanonical signals crucial for *Xenopus* gastrulation (Kim, G. H. et al., 2008).

Downstream of *dishevelled*, the noncanonical Wnt pathway bifurcates into several branches, including into a *daam1*-dependent branch that mediates cytoskeletal reorganization (reviewed in Montcouquiol et al., 2006). We find that in addition to binding MuSK, Dishevelled also colocalizes with and binds to Ankrd6 (previously known as Diversin) and Daam1, two proteins with well-characterized functions in PCP signaling (Habas et al., 2001; Itoh et al., 2009; Kida et al., 2007; Moeller et al., 2006). Daam1 is a member of the Formin family of proteins and is a central player in cytoskeletal reorganization (Alberts, 2002; Wallar and Alberts, 2003), in part through RhoA (Habas et al., 2001), a small GTPase known for its ability to modify the actin cytoskeleton (Maekawa et al., 1999; Matsui et al., 1996). Consistent with this view, we find that inhibiting RhoA function in adaxial muscle cells impairs AChR clustering (supplementary material Fig. S3), although it remains unclear how modifications of the actin cytoskeleton affect AChR clustering during synapse initiation in vivo. In cultured myotubes, actin dynamics have been shown to regulate AChR trafficking and accumulation (Dai et al., 2000; Lee et al., 2009; Pato et al., 2008). Regardless of the precise mechanism, our results demonstrate that core members of the PCP pathway known to regulate cytoskeleton dynamics colocalize with MuSK and play in vivo roles during synapse initiation.

One outstanding question is the mechanism by which Rab11- and MuSK-positive endosomes localize to the center of muscle cells. Rab11 retains its subcellular localization even in the absence of *musk (unp)* and *dishevelled* (supplementary material Fig. S2G), which suggests that muscle cells have an inherent, MuSK-independent 'polarity'. Moreover, Rab7-positive late endosomes are distributed throughout muscle cells, excluding a 'general' endosome localization mechanism. The restricted localization of Rab11 is reminiscent of the situation in *Drosophila* sensory organ precursor (SOP) cells, where Rab11 is localized to only one of two daughter cells following cell division, independent of the Par complex (Emery et al., 2005). Instead, Rab11 localization requires Nuclear fallout (also known as Arfophilin, Eferin or Rab11-FIP3), which has been proposed to provide a link between *rab11* and the dynein light intermediate chain (Horgan et al., 2010). Alternatively, the position of the nucleus might determine Rab11 localization, and thereby synapse position, although altering muscle nuclei position through Syne-1 knockdown does not interfere with neuromuscular synapse maturation (Grady et al., 2005). If *rab11* effector proteins and/or additional factors play a role in the localized accumulation of AChRs and ultimately synapse initiation remains an open question. Nonetheless, our results suggest a basic mechanism by which Wnt signals shape synapse localization through localized receptor endocytosis.

Acknowledgements
Thanks to C. Buckley, G. Gould, T. Schafer, R. Habas, Y. Kida, J. C. Izpisua Belmonte and P. Klein for providing constructs.

Funding
This work was supported by National Science Foundation and National Institutes of Health grants [NIH F31 NS066701 to L.R.G., and NIH R01 HD37975 and NSF 0920336 to M.G.). Deposited in PMC for release after 12 months.

Competing interests statement
The authors declare no competing financial interests.

Supplementary material
Supplementary material available online at
http://dev.biologists.org/lookup/suppl/doi:10.1242/dev.071555/-/DC1

References
Alberts, A. S. (2002). Diaphanous-related Formin homology proteins. *Curr. Biol.* **12**, R796.
Axelrod, J. D., Miller, J. R., Shulman, J. M., Moon, R. T. and Perrimon, N. (1998). Differential recruitment of Dishevelled provides signaling specificity in the planar cell polarity and Wingless signaling pathways. *Genes Dev.* **12**, 2610-2622.
Banerjee, S., Gordon, L., Donn, T. M., Berti, C., Moens, C. B., Burden, S. J. and Granato, M. (2011). A novel role for MuSK and non-canonical Wnt signaling during segmental neural crest cell migration. *Development* **138**, 3287-3296.
Bruneau, E. G. and Akaaboune, M. (2006). The dynamics of recycled acetylcholine receptors at the neuromuscular junction in vivo. *Development* **133**, 4485-4493.
Budnik, V. and Salinas, P. C. (2011). Wnt signaling during synaptic development and plasticity. *Curr. Opin. Neurobiol.* **21**, 151-159.
Campanelli, J. T., Hoch, W., Rupp, F., Kreiner, T. and Scheller, R. H. (1991). Agrin mediates cell contact-induced acetylcholine receptor clustering. *Cell* **67**, 909-916.
Chen, W., Feng, Y., Chen, D. and Wandinger-Ness, A. (1998). Rab11 is required for trans-golgi network-to-plasma membrane transport and a preferential target for GDP dissociation inhibitor. *Mol. Biol. Cell* **9**, 3241-3257.
Chen, W., ten Berge, D., Brown, J., Ahn, S., Hu, L. A., Miller, W. E., Caron, M. G., Barak, L. S., Nusse, R. and Lefkowitz, R. J. (2003). Dishevelled 2 recruits beta-arrestin 2 to mediate Wnt5A-stimulated endocytosis of Frizzled 4. *Science* **301**, 1391-1394.
Ciani, L. and Salinas, P. C. (2005). WNTs in the vertebrate nervous system: from patterning to neuronal connectivity. *Nat. Rev. Neurosci.* **6**, 351-362.
Clarke, M., Ewart, M. A., Santy, L. C., Prekeris, R. and Gould, G. W. (2006). ACRP30 is secreted from 3T3-L1 adipocytes via a Rab11-dependent pathway. *Biochem. Biophys. Res. Commun.* **342**, 1361-1367.
Dai, Z., Luo, X., Xie, H. and Peng, H. B. (2000). The actin-driven movement and formation of acetylcholine receptor clusters. *J. Cell Biol.* **150**, 1321-1334.
Davis, E. and Ghosh, A. (2007). Should I stay or should I go: Wnt signals at the synapse. *Cell* **130**, 593-596.
DeChiara, T. M., Bowen, D. C., Valenzuela, D. M., Simmons, M. V., Poueymirou, W. T., Thomas, S., Kinetz, E., Compton, D. L., Rojas, E., Park, J. S. et al. (1996). The receptor tyrosine kinase MuSK is required for neuromuscular junction formation in vivo. *Cell* **85**, 501-512.
Downes, G. B., Waterbury, J. A. and Granato, M. (2002). Rapid in vivo labeling of identified zebrafish neurons. *Genesis* **34**, 196-202.
Elworthy, S., Hargrave, M., Knight, R., Mebus, K. and Ingham, P. W. (2008). Expression of multiple slow myosin heavy chain genes reveals a diversity of zebrafish slow twitch muscle fibres with differing requirements for Hedgehog and Prdm1 activity. *Development* **135**, 2115-2126.
Emery, G., Hutterer, A., Berdnik, D., Mayer, B., Wirtz-Peitz, F., Gaitan, M. G. and Knoblich, J. A. (2005). Asymmetric Rab 11 endosomes regulate delta recycling and specify cell fate in the Drosophila nervous system. *Cell* **122**, 763-773.
Fan, G. H., Lapierre, L. A., Goldenring, J. R., Sai, J. and Richmond, A. (2004). Rab11-family interacting protein 2 and myosin Vb are required for CXCR2 recycling and receptor-mediated chemotaxis. *Mol. Biol. Cell* **15**, 2456-2469.
Fischbach, G. D. and Cohen, S. A. (1973). The distribution of acetylcholine sensitivity over uninnervated and innervated muscle fibers grown in cell culture. *Dev. Biol.* **31**, 147-162.
Flanagan-Steet, H., Fox, M. A., Meyer, D. and Sanes, J. R. (2005). Neuromuscular synapses can form in vivo by incorporation of initially aneural postsynaptic specializations. *Development* **132**, 4471-4481.
Gagliardi, M., Piddini, E. and Vincent, J. P. (2008). Endocytosis: a positive or a negative influence on Wnt signalling? *Traffic* **9**, 1-9.
Gao, C. and Chen, Y. G. (2009). Dishevelled: the hub of Wnt signaling. *Cell Signal.* **22**, 717-727.
Glass, D. J., Bowen, D. C., Stitt, T. N., Radziejewski, C., Bruno, J., Ryan, T. E., Gies, D. R., Shah, S., Mattsson, K., Burden, S. J. et al. (1996). Agrin acts via a MuSK receptor complex. *Cell* **85**, 513-523.
Godfrey, E. W., Nitkin, R. M., Wallace, B. G., Rubin, L. L. and McMahan, U. J. (1984). Components of Torpedo electric organ and muscle that cause aggregation of acetylcholine receptors on culture muscle cells. *J. Cell Biol.* **99**, 615-627.
Grady, R., Starr, D., Ackerman, G., Sanes, J. and Han, M. (2005). Syne proteins anchor muscle nuclei at the neuromuscular junction. *Proc. Natl. Acad. Sci. USA* **102**, 4359-4364.
Groves, J. A., Hammond, C. L. and Hughes, S. M. (2005). Fgf8 drives myogenic progression of a novel lateral fast muscle fibre population in zebrafish. *Development* **132**, 4211-4222.
Habas, R., Kato, Y. and He, X. (2001). Wnt/Frizzled activation of Rho regulates vertebrate gastrulation and requires a novel Formin homology protein Daam1. *Cell* **107**, 843-854.
Hall, A. C., Lucas, F. R. and Salinas, P. C. (2000). Axonal remodeling and synaptic differentiation in the cerebellum is regulated by WNT-7a signaling. *Cell* **100**, 525-535.
Haribaskar, R., Putz, M., Schupp, B., Skouloudaki, K., Bietenbeck, A., Walz, G. and Schafer, T. (2009). The planar cell polarity (PCP) protein Diversin translocates to the nucleus to interact with the transcription factor AF9. *Biochem. Biophys. Res. Commun.* **387**, 212-217.
Heisenberg, C. P., Tada, M., Rauch, G. J., Saude, L., Concha, M. L., Geisler, R., Stemple, D. L., Smith, J. C. and Wilson, S. W. (2000). Silberblick/Wnt11 mediates convergent extension movements during zebrafish gastrulation. *Nature* **405**, 76-81.
Horgan, C. P., Hanscom, S. R., Jolly, R. S., Futter, C. E. and McCaffrey, M. W. (2010). Rab11-FIP3 links the Rab11 GTPase and cytoplasmic dynein to mediate transport to the endosomal-recycling compartment. *J. Cell Sci.* **123**, 181-191.
Hutagalung, A. H. and Novick, P. J. (2011). Role of Rab GTPases in membrane traffic and cell physiology. *Physiol. Rev.* **91**, 119-149.
Itoh, K., Jenny, A., Mlodzik, M. and Sokol, S. Y. (2009). Centrosomal localization of Diversin and its relevance to Wnt signaling. *J. Cell Sci.* **122**, 3791-3798.
Jing, L., Gordon, L. R., Shtibin, E. and Granato, M. (2010). Temporal and spatial requirements of unplugged/MuSK function during zebrafish neuromuscular development. *PLoS ONE* **5**, e8843.
Jing, L., Lefebvre, J. L., Gordon, L. R. and Granato, M. (2009). Wnt signals organize synaptic prepattern and axon guidance through the zebrafish unplugged/MuSK receptor. *Neuron* **61**, 721-733.
Jing, S., Tapley, P. and Barbacid, M. (1992). Nerve growth factor mediates signal transduction through trk homodimer receptors. *Neuron* **9**, 1067-1079.
Kida, Y. S., Sato, T., Miyasaka, K. Y., Suto, A. and Ogura, T. (2007). Daam1 regulates the endocytosis of EphB during the convergent extension of the zebrafish notochord. *Proc. Natl. Acad. Sci. USA* **104**, 6708-6713.
Kim, G. H., Her, J. H. and Han, J. K. (2008). Ryk cooperates with Frizzled 7 to promote Wnt11-mediated endocytosis and is essential for Xenopus laevis convergent extension movements. *J. Cell Biol.* **182**, 1073-1082.
Kim, N. and Burden, S. J. (2008). MuSK controls where motor axons grow and form synapses. *Nat. Neurosci.* **11**, 19-27.
Kim, N., Stiegler, A. L., Cameron, T. O., Hallock, P. T., Gomez, A. M., Huang, J. H., Hubbard, S. R., Dustin, M. L. and Burden, S. J. (2008). Lrp4 is a receptor for Agrin and forms a complex with MuSK. *Cell* **135**, 334-342.
Klassen, M. P. and Shen, K. (2007). Wnt signaling positions neuromuscular connectivity by inhibiting synapse formation in C. elegans. *Cell* **130**, 704-716.
Lee, C. W., Han, J., Bamburg, J. R., Han, L., Lynn, R. and Zheng, J. Q. (2009). Regulation of acetylcholine receptor clustering by ADF/cofilin-directed vesicular trafficking. *Nat. Neurosci.* **12**, 848-856.
Liebl, F. L., Wu, Y., Featherstone, D. E., Noordermeer, J. N., Fradkin, L. and Hing, H. (2008). Derailed regulates development of the Drosophila neuromuscular junction. *Dev. Neurobiol.* **68**, 152-165.
Lin, W., Burgess, R. W., Dominguez, B., Pfaff, S. L., Sanes, J. R. and Lee, K. F. (2001). Distinct roles of nerve and muscle in postsynaptic differentiation of the neuromuscular synapse. *Nature* **410**, 1057-1064.
Liu, W., Sato, A., Khadka, D., Bharti, R., Diaz, H., Runnels, L. W. and Habas, R. (2008). Mechanism of activation of the Formin protein Daam1. *Proc. Natl. Acad. Sci. USA* **105**, 210-215.
Lucas, F. R. and Salinas, P. C. (1997). WNT-7a induces axonal remodeling and increases synapsin I levels in cerebellar neurons. *Dev. Biol.* **192**, 31-44.
Luo, Z. G., Wang, Q., Zhou, J. Z., Wang, J., Luo, Z., Liu, M., He, X., Wynshaw-Boris, A., Xiong, W. C., Lu, B. et al. (2002). Regulation of AChR clustering by Dishevelled interacting with MuSK and PAK1. *Neuron* **35**, 489-505.
Maekawa, M., Ishizaki, T., Boku, S., Watanabe, N., Fujita, A., Iwamatsu, A., Obinata, T., Ohashi, K., Mizuno, K. and Narumiya, S. (1999). Signaling from Rho to the actin cytoskeleton through protein kinases ROCK and LIM-kinase. *Science* **285**, 895-898.
Martinez-Pena y Valenzuela, I., Mouslim, C. and Akaaboune, M. (2010). Calcium/calmodulin kinase II-dependent acetylcholine receptor cycling at the mammalian neuromuscular junction in vivo. *J. Neurosci.* **30**, 12455-12465.
Matsui, T., Amano, M., Yamamoto, T., Chihara, K., Nakafuku, M., Ito, M., Nakano, T., Okawa, K., Iwamatsu, A. and Kaibuchi, K. (1996). Rho-

associated kinase, a novel serine/threonine kinase, as a putative target for small GTP binding protein Rho. *EMBO J.* **15**, 2208-2216.
Matsui, T., Raya, A., Kawakami, Y., Callol-Massot, C., Capdevila, J., Rodriguez-Esteban, C. and Izpisua Belmonte, J. C. (2005). Noncanonical Wnt signaling regulates midline convergence of organ primordia during zebrafish development. *Genes Dev.* **19**, 164-175.
Merte, J., Jensen, D., Wright, K., Sarsfield, S., Wang, Y., Schekman, R. and Ginty, D. D. (2010). Sec24b selectively sorts Vangl2 to regulate planar cell polarity during neural tube closure. *Nat. Cell Biol.* **12**, 41-46.
Moeller, H., Jenny, A., Schaeffer, H. J., Schwarz-Romond, T., Mlodzik, M., Hammerschmidt, M. and Birchmeier, W. (2006). Diversin regulates heart formation and gastrulation movements in development. *Proc. Natl. Acad. Sci. USA* **103**, 15900-15905.
Montcouquiol, M., Crenshaw, E. B., 3rd and Kelley, M. W. (2006). Noncanonical Wnt signaling and neural polarity. *Annu. Rev. Neurosci.* **29**, 363-386.
Nojima, H., Rothhamel, S., Shimizu, T., Kim, C. H., Yonemura, S., Marlow, F. L. and Hibi, M. (2010). Syntabulin, a motor protein linker, controls dorsal determination. *Development* **137**, 923-933.
Packard, M., Koo, E. S., Gorczyca, M., Sharpe, J., Cumberledge, S. and Budnik, V. (2002). The Drosophila Wnt, wingless, provides an essential signal for pre- and postsynaptic differentiation. *Cell* **111**, 319-330.
Panzer, J. A., Song, Y. and Balice-Gordon, R. J. (2006). In vivo imaging of preferential motor axon outgrowth to and synaptogenesis at prepatterned acetylcholine receptor clusters in embryonic zebrafish skeletal muscle. *J. Neurosci.* **26**, 934-947.
Pato, C., Stetzkowski-Marden, F., Gaus, K., Recouvreur, M., Cartaud, A. and Cartaud, J. (2008). Role of lipid rafts in agrin-elicited acetylcholine receptor clustering. *Chem. Biol. Interact.* **175**, 64-67.
Pitulescu, M. E. and Adams, R. H. (2010). Eph/ephrin molecules-a hub for signaling and endocytosis. *Genes Dev.* **24**, 2480-2492.
Ren, M., Xu, G., Zeng, J., De Lemos-Chiarandini, C., Adesnik, M. and Sabatini, D. D. (1998). Hydrolysis of GTP on rab11 is required for the direct delivery of transferrin from the pericentriolar recycling compartment to the cell surface but not from sorting endosomes. *Proc. Natl. Acad. Sci. USA* **95**, 6187-6192.
Ruegg, M. A., Tsim, K. W., Horton, S. E., Kroger, S., Escher, G., Gensch, E. M. and McMahan, U. J. (1992). The agrin gene codes for a family of basal lamina proteins that differ in function and distribution. *Neuron* **8**, 691-699.
Sato, K. and Nakano, A. (2007). Mechanisms of COPII vesicle formation and protein sorting. *FEBS Lett.* **581**, 2076-2082.
Satoh, A. K., O'Tousa, J. E., Ozaki, K. and Ready, D. F. (2005). Rab11 mediates post-Golgi trafficking of rhodopsin to the photosensitive apical membrane of Drosophila photoreceptors. *Development* **132**, 1487-1497.
Schneider, V. A. and Granato, M. (2006). The myotomal diwanka (lh3) glycosyltransferase and type XVIII collagen are critical for motor growth cone migration. *Neuron* **50**, 683-695.
Shafer, B., Onishi, K., Lo, C., Colakoglu, G. and Zou, Y. (2011). Vangl2 promotes Wnt/planar cell polarity-like signaling by antagonizing Dvl1-mediated feedback inhibition in growth cone guidance. *Dev. Cell* **20**, 177-191.
Sonnichsen, B., De Renzis, S., Nielsen, E., Rietdorf, J. and Zerial, M. (2000). Distinct membrane domains on endosomes in the recycling pathway visualized by multicolor imaging of Rab4, Rab5, and Rab11. *J. Cell Biol.* **149**, 901-914.
Strutt, H. and Strutt, D. (2009). Asymmetric localisation of planar polarity proteins: Mechanisms and consequences. *Semin. Cell Dev. Biol.* **20**, 957-963.
Sytkowski, A. J., Vogel, Z. and Nirenberg, M. W. (1973). Development of acetylcholine receptor clusters on cultured muscle cells. *Proc. Natl. Acad. Sci. USA* **70**, 270-274.
Thermes, V., Grabher, C., Ristoratore, F., Bourrat, F., Choulika, A., Wittbrodt, J. and Joly, J. S. (2002). I-SceI meganuclease mediates highly efficient transgenesis in fish. *Mech. Dev.* **118**, 91-98.
Thisse, C. and Thisse, B. (2005). High throughput expression analysis of ZF-models consortium clones. In *ZFIN Direct Data Submission*
Ullrich, O., Reinsch, S., Urbe, S., Zerial, M. and Parton, R. G. (1996). Rab11 regulates recycling through the pericentriolar recycling endosome. *J. Cell Biol.* **135**, 913-924.
Vieira, A. V., Lamaze, C. and Schmid, S. L. (1996). Control of EGF receptor signaling by clathrin-mediated endocytosis. *Science* **274**, 2086-2089.
Wallar, B. J. and Alberts, A. S. (2003). The formins: active scaffolds that remodel the cytoskeleton. *Trends Cell Biol.* **13**, 435-446.
Wallingford, J. B., Rowning, B. A., Vogeli, K. M., Rothbacher, U., Fraser, S. E. and Harland, R. M. (2000). Dishevelled controls cell polarity during Xenopus gastrulation. *Nature* **405**, 81-85.
Wansleeben, C., Feitsma, H., Montcouquiol, M., Kroon, C., Cuppen, E. and Meijlink, F. (2010). Planar cell polarity defects and defective Vangl2 trafficking in mutants for the COPII gene Sec24b. *Development* **137**, 1067-1073.
Weatherbee, S. D., Anderson, K. V. and Niswander, L. A. (2006). LDL-receptor-related protein 4 is crucial for formation of the neuromuscular junction. *Development* **133**, 4993-5000.
Witzel, S., Zimyanin, V., Carreira-Barbosa, F., Tada, M. and Heisenberg, C. P. (2006). Wnt11 controls cell contact persistence by local accumulation of Frizzled 7 at the plasma membrane. *J. Cell Biol.* **175**, 791-802.
Wu, H., Xiong, W. C. and Mei, L. (2010). To build a synapse: signaling pathways in neuromuscular junction assembly. *Development* **137**, 1017-1033.
Wu, J. and Mlodzik, M. (2009). A quest for the mechanism regulating global planar cell polarity of tissues. *Trends Cell Biol.* **19**, 295-305.
Yang, G. Y., Liang, B., Zhu, J. and Luo, Z. G. (2010). Calpain activation by Wingless-type murine mammary tumor virus integration site family, member 5A (Wnt5a) promotes axonal growth. *J. Biol. Chem.* **286**, 6566-6576.
Yang, X., Li, W., Prescott, E. D., Burden, S. J. and Wang, J. C. (2000). DNA topoisomerase IIbeta and neural development. *Science* **287**, 131-134.
Yang, X., Arber, S., William, C., Li, L., Tanabe, Y., Jessell, T. M., Birchmeier, C. and Burden, S. J. (2001). Patterning of muscle acetylcholine receptor gene expression in the absence of motor innervation. *Neuron* **30**, 399-410.
Yang, X. L., Huang, Y. Z., Xiong, W. C. and Mei, L. (2005). Neuregulin-induced expression of the acetylcholine receptor requires endocytosis of ErbB receptors. *Mol. Cell Neurosci.* **28**, 335-346.
Zeller, J. and Granato, M. (1999). The zebrafish diwanka gene controls an early step of motor growth cone migration. *Development* **126**, 3461-3472.
Zeller, J., Schneider, V., Malayaman, S., Higashijima, S., Okamoto, H., Gui, J., Lin, S. and Granato, M. (2002). Migration of zebrafish spinal motor nerves into the periphery requires multiple myotome-derived cues. *Dev. Biol.* **252**, 241-256.
Zhang, B., Luo, S., Wang, Q., Suzuki, T., Xiong, W. C. and Mei, L. (2008). LRP4 serves as a coreceptor of agrin. *Neuron* **60**, 285-297.
Zhang, J. and Granato, M. (2000). The zebrafish unplugged gene controls motor axon pathway selection. *Development* **127**, 2099-2111.
Zhang, J., Lefebvre, J. L., Zhao, S. and Granato, M. (2004). Zebrafish unplugged reveals a role for muscle-specific kinase homologs in axonal pathway choice. *Nat. Neurosci.* **7**, 1303-1309.
Zhu, D., Yang, Z., Luo, Z., Luo, S., Xiong, W. C. and Mei, L. (2008). Muscle-specific receptor tyrosine kinase endocytosis in acetylcholine receptor clustering in response to agrin. *J. Neurosci.* **28**, 1688-1696.